Rapid differentiation of SARS-CoV-2 variants on a nanotechnology enhanced DNA-chip

Hongjie Dai (hdai@stanford.edu)
Stanford University https://orcid.org/0000-0002-4906-4502

Ying Liu
Southern University of Science and Technology

Yang Yang
Shenzhen Third People's Hospital

Guanghui Wang
Southern University of Science and Technology

Ruibin Hu
Southern University of Science and Technology

Pan-Lin Shao
Guangzhou Medical University

Jiahu Tang
Southern University of Science and Technology

Ziyi Xu
Southern University of Science and Technology

Yan Liu
Shenzhen Third People's Hospital

Hongjun Xiao
Southern University of Science and Technology

Jiahui Lv
Southern University of Science and Technology

Jingkai Yang
Southern University of Science and Technology

Dan Niu
Southern University of Science and Technology

Tang Meijie
Nirmidas Biotech Inc. https://orcid.org/0000-0003-3432-4479

Jing Yuan
Shenzhen Third People's Hospital

Bo Zhang
Southern University of Science and Technology

Biological Sciences - Article

Keywords:

Posted Date: May 24th, 2022

DOI: https://doi.org/10.21203/rs.3.rs-1641024/v1

Abstract

With the persistence of the COVID-19 pandemic caused primarily by constant viral mutations, rapid identification of different lineages of severe acute respiratory syndrome coronavirus 2 (SARS-CoV-2) by large-scale screening at the point-of-care could be key to monitoring and assessing viral evolutions. Herein, we developed a Fluorescence Enhanced Microarray for Multiplex Analysis of Nucleic acids (FEMMAN) for detecting 8 SARS-CoV-2 variants simultaneously in ~ 3 hours without the need of RNA extraction, opening the possibility of point-of-care testing of multiple SARS-CoV-2 variants while reducing the cost significantly to ~ $ 7 per sample from ~ $100 by Next-Generation Sequencing (NGS). Combined with isothermal amplification, the multiplexed RNA assay achieved single-copy detection sensitivity and single nucleotide variant (SNV) distinction owing to the nanotechnology based plasmonic gold (pGOLD) near-infrared fluorescence enhancing platform. Probing 10 targets of three mutational hotspots in S gene, we differentiated 8 viral lineages (Wild type, Alpha, Beta, Gamma, Delta, Lambda, Mu, and Omicron) of SARS-CoV-2, validated using nasopharyngeal swabs obtained from 127 individuals, achieving a 100% sensitivity and 100% specificity in SARS-CoV-2 detection, and a 91.1% concordance with NGS in variant identification. The scalable, multiplexed FEMMAN assay could shift the paradigm of COVID-19 diagnostic and surveillance from positive/negative assessments to simultaneous lineage identification in large-scale screening, greatly facilitating the global monitoring of SARS-CoV-2 variants.

Full Text

In the past two years, the COVID-19 pandemic caused by the spread of SARS-CoV-2 has led to billions of infections and over six million deaths worldwide as of May 2022[1]. The global infectious disease surveillance system has been challenged by the rapid spreading of the virus, as well as the shortage of reagents and equipment[2]. With the continuous emergence of SARS-CoV-2 variants induced by frequent mutations altering viral pathogenicity, infectivity, transmissibility, and antigenicity[3], we are in urgent need of high-throughput, sensitive, and multiplexed point-of-care technologies to rapidly detect SARS-CoV-2 mutations and identify the viral lineages during large-scale screening[4].

Currently, the SARS-CoV-2 viral RNA diagnostic approaches were mostly based on quantitative reverse transcription PCR (RT-qPCR)[5], clustered regularly interspaced short palindromic repeats (CRISPR)[6], or sequencing[7]. Restricted by limited fluorescent channels, most qPCR-based approaches, though high-throughput, can only detect less than 4 targets[8]. The CRISPR-based approaches revolutionized SARS-CoV-2 diagnostic by improving the portability, cost-efficiency, and rapidity while being able to detect only one or a small number of targets in a given reaction[9,10]. Recently, a CRISPR-based assay combined with microfluidic technology achieved multiplexed nucleic acids detection, though it was complex in design and relied on expensive equipment[11,12]. Next-Generation Sequencing (NGS) is powerful to differentiate SARS-CoV-2 variants, but is difficult to integrate into large-scale screening due to high cost (at least $ 100) and time-consuming (around 3 days) procedures[13].

Fluorescence enhanced microarray technology enables detection of multiplex targets in one reaction[14,15]. In recent years, we have been pursuing the development of a plasmonic gold (pGOLD) chip for multiplexed protein or antibody biomarkers analysis with down to femto-molar sensitivity[16-18]. Owing to the surface plasmonic resonance (SPR) and local electric field enhancement effect, the pGOLD platform affords near-infrared (NIR) fluorescence enhancement to more than 100-fold[19], and has been employed for the diagnosis of Type I Diabetes[16], Zika virus[17], and SARS-CoV-2[18]. However, the pGOLD platform has not been investigated for nucleic acid detection previously.

Here we developed multiplexed viral RNA detection on the pGOLD platform, establishing a rapid and cost-effective diagnostic method, Fluorescence Enhanced Microarray for Multiplex Analysis of Nucleic acids (FEMMAN), for SARS-CoV-2 detection with variant differentiation suitable for large-scale screening. We devised a new surface layering to maximize fluorescence enhancement of the pGOLD substrate, optimized the testing procedures by introducing isothermal amplification and exonuclease digestion with a set of probes and primers design, and replaced complex RNA extraction steps with simple thermal lysis for point-of-care testing (Fig. 1a). Through probing 10 targets of three mutational hotspots (G142-Y145, K417, L452) in S gene (Fig. 1a, b), FEMMAN achieved high-throughput, rapid and multiplexed nucleic acid detection with single-molecule sensitivity (post amplification) and single nucleotide variant (SNV) discrimination (Fig. 1c) for the differentiation of 8 SARS-CoV-2 lineages (Wild type, Alpha, Beta, Gamma, Delta, Lambda, Mu, and Omicron, Fig. 1d). Importantly, with 90 SARS-CoV-2 infected patients, our assay reached 100% sensitivity and 100% specificity in SARS-CoV-2 diagnosis, and a 91.1% concordance with NGS in variant identification. Further, the assay can be easily expanded to tens of SARS-CoV-2 variants and generalized for the detection of other viruses and variants.

For nucleic acids detection by FEMMAN on the pGOLD substrate, we found that the fluorescence enhancement on pGOLD is positively correlated with the distance between detection fluorophore and pGOLD substrate within a certain limit (Extended Data Fig. 1c, d). Our optimization found that a compact bovine serum albumin (BSA) layer on pGOLD provided sufficient free NH_2 groups for sulfosuccinimidyl-4-(*N*-maleimidomethyl) cyclohexane-1-carboxylate (sulfo-SMCC) assembly for efficient thiolated DNA probe immobilization while affording the highest fluorescence signal enhancement (Extended Data Fig. 1a). The BSA layer on pGOLD was also beneficial to protect gold nanostructures from being etched by the condensed thiol groups on the DNA probes (Extended Data Fig. 1c, d), inhibit the non-specific binding of biomolecules from samples, and provide sufficient reactive sites for thiolated DNA probes[20]. Post DNA probes immobilization, the established FEMMAN chip was incubated with biotinylated single-stranded DNA target in binding buffer (binding buffer optimization see Extended Data Fig. 1e), followed by identification with IRDye800 labeled streptavidin (Extended Data Fig. 1b), yielded fluorescence-based detection limit of ~ 2 fM with dynamic range from 2 fM to 200 pM (Extended Data Fig. 2) without template amplification. Compared to traditional DNA microarray on glass substrate, plasmonic gold film boosts IRDye800 fluorescence intensity by > 1,000-fold, resulting in sensitivity improvement from 2 pM to 2 fM prior target amplification (Extended Data Fig. 2).

Although our analytical sensitivity for nucleic acid detection on pGOLD is a significant improvement over previous studies with DNA microarray on glass substrate, atto-molar sensitivity is required for SARS-CoV-2 diagnostics[21]. We explored combining FEMMAN assay with isothermal amplification. Of the methods explored, Recombinase Polymerase Amplification (RPA)[22] afforded high sensitivity with minimal sample preparation and compatibility with reverse transcriptase (RT) to convert RNA to DNA for amplification[23]. More importantly, as only two primers are required, multiplexing is relatively simple for RPA, facilitating our development of multiplexed nucleic acids detection with atto-molar sensitivity by FEMMAN-RPA. The samples were amplified by RT-RPA with 5’-biotin labeled forward primers and 5’-phosphorylated reverse primers, followed with digestion by Lambda Exonuclease (Lambda Exo), which selectively digests the 5'-phosphorylated strand of double-stranded DNA (unless otherwise noted, all FEMMAN-RPA assays performed these two steps, with the single-stranded amplicon in binding buffer directly added to the FEMMAN chip without further purification). We also performed asymmetric RPA[24] to gain single-stranded amplified sample, and attained inferior detection sensitivity. Nevertheless, this simplified alternative route is suitable for detections of which single copy sensitivity is not required (Extended Data Fig. 3).

FEMMAN-RPA is sensitive, specific, scalable and easy-to-operate. We achieved SARS-CoV-2 detection with single-copy sensitivity post isothermal amplification, as verified by digital-droplet PCR (ddPCR), matching the sensitivity of specific high-sensitivity enzymatic reporter unlocking (SHERLOCK)[6] and PCR-based assay[5]. We selected N501, a hotspot mutation site in SARS-CoV-2 variants, as target site to evaluate the performance of FEMMAN-RPA assay (Fig. 2a). The probes and primers were designed according to the sequence of N501 site and bilateral conserved regions (Fig. 2b). According to the optimized condition, single digit copies sensitivity was achieved using FEMMAN assay post amplification (Fig. 2c, d), which could not be realized using conventional glass slides (Fig. 2c).

We next examined the specificity of FEMMAN assay. First, the specificity of FEMMAN was demonstrated through probing 15-plexed DNA microarray without template amplification (Extended Data Fig. 4a). Sensitivity of DNA detection in the multiplexed array was the same as single DNA detection, with fluorescence signal on non-specific DNA probe at background level (Extended Data Fig. 4b). The fluorescence intensities on single and double nucleotide mismatch version were only ~ 10% and 5% of intensity on match version, demonstrating the capability of FEMMAN chip in SNV discrimination (Extended Data Fig. 4c). Combining with the high conservation of amplification by RT-RPA, FEMMAN achieved target identification with down to single-digit copies sensitivity post amplification and SNV discrimination (Extended Data Fig. 2c, d), laying the foundation for simultaneous discrimination of SARS-CoV-2 variants.

Accurate identification of SARS-CoV-2 lineage in large-scale screening requires simultaneous differentiation of multiple RNA mutation sites with high throughput. To achieve this goal, we assembled all target sites identification in one assay for each sample. A SARS-CoV-2 panel covering three distinctive mutation sites (G142-Y145, K417, L452) of the Spike protein (S protein) was designed for FEMMAN-RPA assay (Fig. 3a, b). Containing the receptor binding domain (RBD), the sequence of S protein is specific for

SARS-CoV-2[25]. The mutations on S protein were associated with more serious symptoms, increased transmissibility, significant reduction in neutralization by antibodies or reduced effectiveness of treatments or vaccines[26]. Some specific variants are in the spotlight and require more appropriate public health actions. As for G142-Y145, K417, and L452 sites, there are more than 2 mutation types for each site in different SARS-CoV-2 variants[27-29]. The viral lineage can be identified with permutation and combination of the 3 mutation sites.

We first tested the SARS-CoV-2 panel and evaluated its performance with synthetic viral RNA of wild type and B.1.617.2 (Delta) variant (Extended Data Fig. 5, see methods for details). To evaluate the accuracy of FEMMAN-RPA for SARS-CoV-2 lineages identification, lentiviruses harboring genome fragments of S protein for SARS-CoV-2 wild type, B.1.1.7 (Alpha), B.1.351 (Beta), P.1 (Gamma), B.1.617.2 (Delta), C.37 (Lambda), B.1.621 (Mu), and B.1.1.529 (Omicron) variants were constructed. The extracted RNA of lentivirus was used as template for triplex RT-RPA targeting G142-Y145, K417 and L452 sites, followed with viral lineage discrimination by FEMMAN (Extended Data Fig. 5d, see Methods for details). The fluorescence images (Fig. 3c) and statistical heat map (Fig. 3d) for 8 SARS-CoV-2 lineages obtained by FEMMAN-RPA clearly demonstrated its capability in viral lineages discrimination with SNV distinction.

Next, we show that FEMMAN-RPA is an effective point-of-care technology. As a single-stranded and positive-sense RNA virus, the RNA in SARS-CoV-2 is incompact[30] compared to genomic DNA, which exists as highly compacted nucleosome arrays[31]. The viral RNA would be released by disrupting the envelope and nucleocapsid of the virus through chemical lysis, protease digestion or thermal lysis[32]. To simulate clinical application without nucleic acid extraction, we performed FEMMAN-RPA assay using thermal lysed lentivirus in preservation solution (Fig. 3e, see methods for details). In contrast with the blank using buffer only as input, FEMMAN-RPA achieved single-RNA copy sensitivity post amplification without viral RNA extraction (Fig. 3f), a clear improvement over qPCR (Fig. 3g). Compared with extracted viral RNA, using the thermal lysed sample as input faced challenges of the impurities mainly consist of various proteins in the sample. Owing to the high analytical sensitivity and minimal sample load required by FEMMAN-RPA assay, the impurities were significantly diluted to having negligible influence on the amplification system. Replacing viral RNA extraction steps/equipment with a simple water bath, FEMMAN-RPA is suitable for point-of-care testing and allows identification of SARS-CoV-2 lineages in 3 hours after swab collection (wild type see Fig. 1c, Alpha sees Fig. 3h, other variants see Extended Data Fig. 6).

Finally, we evaluated FEMMAN-RPA assay using both thermal lysed nasopharyngeal swab samples and extracted RNA from 127 recruited clinical samples including 28 individuals who had not been infected with SARS-CoV-2, 9 patients infected with other human-associated viruses (HVs, including human coronavirus HCoV-NL63 & HCoV-OC43, influenza A virus H3N2 & H1N1, influenza B virus Yamagata & Victoria subtypes, human adenovirus serotype 3, 7, & 55), 90 samples infected with different lineages of SARS-CoV-2 (identified by NGS, including 76 clinical samples and 14 viral supernatant cultured from clinical samples). For the 76 clinical samples, 49 samples were in the form of extracted RNA, 10 samples

were in the form of thermal lysed nasopharyngeal swab samples, and 17 samples were obtained in both forms. The clinical samples were prepared for FEMMAN-RPA assay, qPCR assay for N, Orb1 and S gene, and Sanger sequencing for S protein. Only 1 μL to 2.5 μL clinical sample was applied as template for FEMMAN-RPA assay according to the procedure (Fig. 4a, see methods for details). We obtained the statistical graph with the sum of the mean fluorescence intensity of G142-Y145 site as the x-axis, K417 site as the y-axis, and L452 site as the z-axis (Fig. 4b). The dots in black and grey represent uninfected individuals and non-SARS-CoV-2 HVs-infected patients respectively. Dots in other colors represent patients infected with different SARS-CoV-2 lineages (red for wild type, yellow for Alpha, blue for Beta, green for Delta, purple for Omicron). Based on a signal threshold of 3 × s.d. above blank, FEMMAN-RPA achieved 100% sensitivity and 100% specificity for SARS-CoV-2 detection, better than qPCR with threshold of Ct = 35 according to the instruction (Fig. 4c).

We further evaluated the specificity of variant identification with the SARS-CoV-2 panel for clinical samples. The viral lineages of 90 clinical samples were tested by NGS, Sanger sequencing of the M1-Y612 fragments for S protein and FEMMAN-RPA assay. We calculated the proportion of the signal for Y144del, Y144SY145N, G142D143-145del, K417N, K417T, L452R, L452Q mutation sites and drew the heat map (Fig. 4f), attaining 91.1% (82 of 90) concordance of FEMMAN-RPA with NGS results (Fig. 4d). Compared with the 77.8% (70 of 90) concordance between Sanger sequencing and NGS (Fig. 4d), our FEMMAN-RPA assay achieved superior specificity to Sanger sequencing. For the 82 samples confirmed by FEMMAN-RPA assay, the detected signals on the multiplexed mutation sites (Y144del for Alpha, K417N for Beta and Omicron, L452R for Delta, and G142D143-145del for Omicron) clearly revealed the viral lineages for each clinical samples (Fig. 4e for 72 samples of extracted RNA, Fig. 4g for 27 samples of thermal lysis), in ~ 91% accordance with NGS. The increase of the L452R signal in Omicron was potentially owing to the interference by adjacent mutations, G446S and N440K, which restrained the perfect match of the forward primer to template. For the samples lineage-unconfirmed by FEMMAN-RPA, the fluorescence intensity of each probe was insufficient to differentiate the viral lineage due to deficient amount of template (<10 copies). Further augmenting the amount of the template applied to RT-RPA has been verified to improve the specificity for samples with low viral load.

To demonstrate that the use of thermal lysis had no influence on the sensitivity and specificity of FEMMAN-RPA assay, we analyzed the concordance of the 17 specimens in both forms. Compared with extracted RNA, the fluorescence signals for G142-Y145, K417 and L452 sites of thermal lysed samples were mostly comparable, even stronger in some specimens (Fig. 4h). The SARS-CoV-2 lineage was clearly identified by FEMMAN-RPA in both forms for all the 17 specimens (Fig. 4e, g). It was worth noting that 10 thermally lysed specimens were not detected by Sanger sequencing, while the lineages were clearly identified by FEMMAN-RPA (Fig. 4g, Omicron). Due to impurities in nasopharyngeal swab samples and viral RNA winding on ribonucleoproteins[30], viral RNA extraction steps were typically required for RT-qPCR and sequencing. Our correlation data here showed that FEMMAN-RPA with thermal lysis achieved similar sensitivity and specificity to without RNA extraction, providing a more holistic point-of-care diagnosis approach to the public.

In summary, we developed a scalable, versatile, and robust platform for multiplexed nucleic acid detection with high sensitivity and specificity. The application for SARS-CoV-2 lineage identification without viral RNA extraction demonstrated its diagnostic and surveillance capabilities for clinical use in global monitoring of the SARS-CoV-2 virus and its variants. The design of FEMMAN chip and the streamlined workflow make FEMMAN a high-throughput and multiplex nucleic acid detection technology. Furthermore, FEMMAN enabled the addition and optimization of new amplification primers or probes to existing SARS-CoV-2 panel to facilitate the detection of emerging variants or other virus in the future, without sample type limitation. Point-of-care testing outside of the clinical diagnostic laboratory, especially in regions with insufficient resources and medical care, could be achieved. FEMMAN provided a novel approach for high-throughput multiplex nucleic acid detection with enhanced sensitivity and superior specificity, correspondingly lowering the reagent and sample consumption per test (Extended Data Table 1) with a broader dynamic range. In the future, FEMMAN is expected to perform multiplexed identification of even more SARS-CoV-2 lineages in large-scale screening, without the acquisition of personal genetic information to track the ongoing evolution of the virus, while reaching more comprehensive diagnostic and surveillance applications for the potential emergence of new variants.

References

1 *Coronavirus disease 2019 (COVID-19) Situation Dashboard* (2022).

2 Mina, M. J. & Anderson, K. G. COVID-19 testing: One size does not fit all. *Science* **371**, 126-127 (2020).

3 Harvey, W. T. *et al.* SARS-CoV-2 variants, spike mutations and immune escape. *Nat. Rev. Microbiol.* **19**, 409-424, doi:10.1038/s41579-021-00573-0 (2021).

4 Rasmussen, A. L. & Popescu, S. V. SARS-CoV-2 transmission without symptoms. *Science* **371**, 1206-1207 (2021).

5 Jin, Y. H. *et al.* A rapid advice guideline for the diagnosis and treatment of 2019 novel coronavirus (2019-nCoV) infected pneumonia (standard version). *Mil. Med. Res.* **7**, 4, doi:10.1186/s40779-020-0233-6 (2020).

6 Gootenberg, J. S. *et al.* Nucleic acid detection with CRISPR-Cas13a/C2c2. *Science* **356**, 438-442 (2017).

7 Park, S. Y., Faraci, G., Ward, P. M., Emerson, J. F. & Lee, H. Y. High-precision and cost-efficient sequencing for real-time COVID-19 surveillance. *Sci. Rep.* **11**, 13669, doi:10.1038/s41598-021-93145-4 (2021).

8 Kudo, E. *et al.* Detection of SARS-CoV-2 RNA by multiplex RT-qPCR. *PLoS Biol.* **18**, e3000867, doi:10.1371/journal.pbio.3000867 (2020).

9 Ding, X. *et al.* All-in-One Dual CRISPR-Cas12a (AIOD-CRISPR) Assay: A Case for Rapid, Ultrasensitive and Visual Detection of Novel Coronavirus SARS-CoV-2 and HIV virus. *bioRxiv*, doi:10.1101/2020.03.19.998724 (2020).

10 Patchsung, M. *et al.* Clinical validation of a Cas13-based assay for the detection of SARS-CoV-2 RNA. *Nat. Biomed. Eng.* **4**, 1140-1149, doi:10.1038/s41551-020-00603-x (2020).

11 Welch, N. L. *et al.* Multiplexed CRISPR-based microfluidic platform for clinical testing of respiratory viruses and identification of SARS-CoV-2 variants. *Nat. Med.*, doi:10.1038/s41591-022-01734-1 (2022).

12 Ackerman, C. M. *et al.* Massively multiplexed nucleic acid detection with Cas13. *Nature* **582**, 277-282, doi:10.1038/s41586-020-2279-8 (2020).

13 Meredith, L. W. *et al.* Rapid implementation of SARS-CoV-2 sequencing to investigate cases of health-care associated COVID-19: a prospective genomic surveillance study. *Lancet Infect. Dis.* **20**, 1263-1271, doi:10.1016/s1473-3099(20)30562-4 (2020).

14 Kuno, A. *et al.* Evanescent-field fluorescence-assisted lectin microarray: a new strategy for glycan profiling. *Nat. Methods* **2**, 851-856 (2005).

15 Badshah, M. A., Ju, J., Lu, X., Abbas, N. & Kim, S.-m. Enhancing the sensitivity of DNA microarrays by metal-enhanced fluorescence using vertical nanorod structures. *Sens. Actuators B Chem.* **274**, 451-457, doi:10.1016/j.snb.2018.07.163 (2018).

16 Zhang, B., Kumar, R. B., Dai, H. & Feldman, B. J. A plasmonic chip for biomarker discovery and diagnosis of type 1 diabetes. *Nat. Med.* **20**, 948-953, doi:10.1038/nm.3619 (2014).

17 Zhang, B. *et al.* Diagnosis of Zika virus infection on a nanotechnology platform. *Nat. Med.* **23**, 548-550, doi:10.1038/nm.4302 (2017).

18 Liu, T. *et al.* Quantification of antibody avidities and accurate detection of SARS-CoV-2 antibodies in serum and saliva on plasmonic substrates. *Nat. Biomed. Eng.* **4**, 1188-1196, doi:10.1038/s41551-020-00642-4 (2020).

19 Koh, B. *et al.* Visible to Near-Infrared Fluorescence Enhanced Cellular Imaging on Plasmonic Gold Chips. *Small* **12**, 457-465, doi:10.1002/smll.201502182 (2016).

20 Zhang, B. *et al.* Multiplexed cytokine detection on plasmonic gold substrates with enhanced near-infrared fluorescence. *Nano Res.* **6**, 113-120, doi:10.1007/s12274-012-0286-2 (2012).

21 Song, L. *et al.* Direct detection of bacterial genomic DNA at sub-femtomolar concentrations using single molecule arrays. *Anal. Chem.* **85**, 1932-1939, doi:10.1021/ac303426b (2013).

22 Piepenburg, O., Williams, C. H., Stemple, D. L. & Armes, N. A. DNA detection using recombination proteins. *PLoS Biol.* **4**, e204, doi:10.1371/journal.pbio.0040204 (2006).

23 Qian, J. *et al.* An enhanced isothermal amplification assay for viral detection. *Nat. Commun.* **11**, 5920, doi:10.1038/s41467-020-19258-y (2020).

24 Kersting, S., Rausch, V., Bier, F. F. & von Nickisch-Rosenegk, M. Multiplex isothermal solid-phase recombinase polymerase amplification for the specific and fast DNA-based detection of three bacterial pathogens. *Mikrochim. Acta* **181**, 1715-1723, doi:10.1007/s00604-014-1198-5 (2014).

25 Huang, Y., Yang, C., Xu, X. F., Xu, W. & Liu, S. W. Structural and functional properties of SARS-CoV-2 spike protein: potential antivirus drug development for COVID-19. *Acta Pharmacol. Sin.* **41**, 1141-1149, doi:10.1038/s41401-020-0485-4 (2020).

26 Gobeil, S. M. *et al.* Effect of natural mutations of SARS-CoV-2 on spike structure, conformation, and antigenicity. *Science* **373**, 5, doi:10.1126/science.abi6226 (2021).

27 Cosar, B. *et al.* SARS-CoV-2 Mutations and their Viral Variants. *Cytokine Growth Factor Rev.* **63**, 13, doi:10.1016/j.cytogfr.2021.06.001 (2021).

28 Xie, X. *et al.* Emerging SARS-CoV-2 B.1.621/Mu variant is prominently resistant to inactivated vaccine-elicited antibodies. *Zool. Res.* **42**, 789-791, doi:10.24272/j.issn.2095-8137.2021.343 (2021).

29 Ren, S. Y., Wang, W. B., Gao, R. D. & Zhou, A. M. Omicron variant (B.1.1.529) of SARS-CoV-2: Mutation, infectivity, transmission, and vaccine resistance. *World J. Clin. Cases* **10**, 1-11, doi:10.12998/wjcc.v10.i1.1 (2022).

30 Yao, H. *et al.* Molecular Architecture of the SARS-CoV-2 Virus. *Cell* **183**, 730-738 e713, doi:10.1016/j.cell.2020.09.018 (2020).

31 Segal, E. *et al.* A genomic code for nucleosome positioning. *Nature* **442**, 8 (2006).

32 Islam, M. S., Aryasomayajula, A. & Selvaganapathy, P. R. A Review on Macroscale and Microscale Cell Lysis Methods. *Micromachines* **8**, 83 (2017).

Methods

FEMMAN chip preparation

Surface chemical modification on pGOLD chip

The pGOLD chips, provided by Nirmidas Biotech, were immersed in Phosphate Buffer Saline (PBS, Lablead) containing 200 mg/mL bovine serum albumin (BSA, Sigma Aldrich) for 2 h, resulting in a dense layer of BSA on pGOLD substrate. After rinsing with PBS buffer and water, the slides were then immersed

into 1 mM Sulfosuccinimidyl 4-[*N*-maleimidomethyl] cyclohexane-1-carboxylate (Sulfo-SMCC, HWRK Chem) in water for 1 h, resulting in a layer of maleimide groups ready to react with thiol functionalized DNA probe[33].

To regulate the distance between detection fluorophore and plasmonic gold film, we constructed a series of surface chemical modification on pGOLD substrate with 1 mM cysteamine (Sigma) in water, 1 mM mercapto-poly(ethylene glycol)-amine (HS-PEG-NH_2, Mw = 1,000, Peng Sheng Biological) in water, 1 mM HS-PEG-NH_2 (Mw = 5,000, Peng Sheng Biological) in water, or 200 mg/mL BSA in PBS buffer, following with 1 mM sulfo-SMCC. The comparison results of background signal and fluorescence intensity for naked pGOLD substrate, different surface chemical modification and glass substrate were listed in Extended Data Fig. 1c, d.

Comparison of plasmonic gold film, evaporated gold film and glass substrate

The glass slides used in comparison were purchased from Fisher Scientific. Evaporated gold film on glass slides were deposited *via* e-beam evaporation with Innotec ES26C E-Beam Evaporator. The pGOLD chips and evaporated gold slides were immersed in 200 mg/mL BSA solution in PBS buffer following with 1 mM Sulfo-SMCC before DNA probe immobilization. Glass slides were immersed into 1 mM (3-Aminopropyl)triethoxysilane (APTES, Sigma) in ethanol overnight[34]. After rinsing and drying, the amine modified glass slides were treated with 1 mM Sulfo-SMCC in water to form a layer of maleimide groups before DNA probe immobilization.

DNA microarray arraying

The maleimide activated slides described above were loaded into Nano-Plotter™ 2.0 (GeSiM mbH) where 2 μM thiolated DNA probe in TE buffer (10 mM Tris-HCl, pH 7.5, 1 mM EDTA, Coolabor) with 25 mM Tris(2-carboxyethyl)phosphine (TCEP, Meryer)[35], 0.01% Tween 20 (Solarbio) and 0.1% Glycerol (Aladdin) was arrayed using Nano Tip J (GeSiM mbH) at 25 °C, resulting in microarray feature with diameters of ~ 400 μm. Typically, each slide was segmented into 16 blocks with a 8 × 2 fashion and each block contained triplicate spots of different probes. After arraying, the slides were stored in humid chamber for 2 h to complete the reaction, dried in a desiccator and then blocked with 0.01% mercapto-hexanol (Macklin) to quench free maleimide groups. The established FEMMAN chips could be stored at 4 °C. The FEMMAN assay affords throughput of 56 samples in one set (Extended Data Fig. 7, 14 blocks in a chip and 4 chips in a frame).

Dynamic range and sensitivity of FEMMAN assay

Synthetic DNA targets

Biotin labeled synthetic DNA targets were ordered from Sangon Biotech and resuspended in DNase/RNase-free water. The resuspended DNA solution was serially diluted from 2 nM to 2 fM in binding buffer and used as inputs to FEMMAN chip.

DNA microarray processing

100 μL of each biotinylated DNA solution (2 nM to 2fM) in binding buffer (TE buffer with 1 M NaCl) was applied to each set of DNA microarray in FEMMAN chip, incubated at room temperature for 1 h to overnight. The chip was washed with TE buffer for 3 times, followed by blocking with 200 mg/mL BSA in PBS buffer and incubated with IRDye800 (Licor Biosciences) or Cy5 (GLPBIO) labeled streptavidin in PBS buffer with 200 mg/mL BSA, the incubation lasted for 30 min at room temperature in dark. Chips were washed for 3 times with PBS-Tween 20 (0.05%) buffer, followed by brief immersion in water and subsequent drying with centrifuge.

For binding buffer optimization, we screened TE buffer with 0.1 M NaCl, TE buffer with 0.5 M NaCl, TE buffer with 1M NaCl, TE buffer with 0.1 M $MgCl_2$, TE buffer with 0.5 M $MgCl_2$, TE buffer with 1 M NaCl and 0.1 M $MgCl_2$, TE buffer with 0.5 M KH_2PO_4, TE buffer with 0.5 M K_2HPO_4, 2 × saline sodium citrate (SSC) buffer, 5 × SSC buffer, 6 × SSC buffer, 6 × SSC buffer with 0.1 M NaCl, 6 × SSC buffer with 1 M NaCl, 6 × SSC buffer with 0.1 M $MgCl_2$, 6 × SSC buffer with 0.5 M KH_2PO_4, 6 × SSC buffer with 0.5 M K_2HPO_4 (Extended Data Fig. 1e).

Microarray scanning and wide field imaging

The commercial MidaScan-IR™ dual-channel confocal scanner (Nirmidas Biotech) was used to scan the IRDye800 or Cy5 labeled microarrays on different substrates with the 785 nm channel for IRDye800 and 670 nm channel for Cy5 with the gain set to 40 as defined by the system. Microarray fluorescence images were analyzed by built-in software of the scanner, and the spot features were automatically identified by the software. The fluorescence intensity of each spot was background subtracted, and the average of median pixel intensity values for each probe arrayed in triplicates was used to represent signal intensity.

Single-fluorophore imaging was performed on Cy5-labed DNA at varying concentrations on both plasmonic substrates and quartz slides. Imaging was done using a 658 nm laser diode excitation source with an 80 μm spot focused with a 100 × lens (Olympus). The excitation light was filtered through a 750 nm short pass filter (Thorlabs) as well as a 655 nm/40 nm bandpass filter (Semrock). The resulting NIR images were collected using an 800 nm short pass filter as well as a 715 nm/40 nm bandpass filter (Semrock) on a 1344 × 1024 pixel silicon CCD camera (Hamamatsu). A binning of 4 and an exposure time of 400 ms was used to obtain videos of varying target DNA concentrations on both the plasmonic and gold substrates. Initial frames were selected to demonstrate the starting Cy5 fluorescent intensity and fluorophore density.

FEMMAN-RPA assay for SARS-CoV-2 detection

Synthetic viral RNA targets

Reference material for SARS-CoV-2 wild type Genomic RNA was purchased from GeneWell Biotechnology Co., Ltd, reference material for SARS-CoV-2 Delta Variant (B.1.617.2) Genomic RNA was purchased from

National Institute of Metrology.

Lentivirus Preparation and Processing

Lentiviruses containing RNA fragments for Spike protein of SARS-COV-2 wild type, B.1.1.7 (Alpha), B.1.351 (Beta), P.1 (Gamma), B.1.617.2 (Delta), C.37 (Lambda), and B.1.621 (Mu) variants were constructed by GeneCopoeia™. Lentivirus containing RNA fragments of Spike protein of B.1.1.529 (Omicron) was constructed by General Biol. Pseudotyped lentiviral particles were titrated using qRT-PCR to determine the physical copy numbers of viral genomic RNA. The lentiviral particles were generated according to standardized protocol using highly purified plasmids and EndoFectin-Lenti™ and TiterBoost™ reagents. The lentiviral transfer vector pEZ-Lv201 was co-transfected into 293Ta cells with Lenti-Pac™ HIV packaging mix. The lentivirus particles were purified and stored at -80 °C in aliquots (purified particles). The construction of lentiviral expression was validated by full-length sequencing, restriction enzyme digestion and PCR-size validation using gene-specific and vector-specific primers. For FEMMAN-RPA assay, the lentiviruses were spiked into the nasopharyngeal swab sample preservation solution (Biocomma®, YMJ15C) and serially diluted, the titer of lentiviruses was determined by ddPCR. 1,000 copies of each lentivirus were spiked into the sample preservation solution respectively for subsequent viral RNA extraction with QIAamp Viral RNA minikit (Qiagen), serially diluted lentiviruses were thermal lysed at 95 °C for 2 min before being used as input for RPA.

Clinical samples

For clinical nasopharyngeal swab samples, RNA was extracted from 140 μL input material using QIAamp Viral RNA minikit (Qiagen) according to the manufacturer's instructions. Samples were eluted in 80 μL of nuclease free water and stored at -80 °C until use. For thermal lysis, the clinical sample was heated at 95 °C for 2 min and used immediately.

Reverse Transcription Recombinase Polymerase Amplification (RT-RPA)

The design principle of Primers for RPA was described in Supplementary Discussion 5. The effect factors include the amplicon size (between 80 and 90 nt), primer melting temperatures (between 54 °C and 67 °C), and primer size (between 30 and 35 nt)[23]. Forward primers were ordered as 5' terminal biotin modified DNA, and reverse primers were ordered as 5' terminal phosphate modified DNA (Sangon Biotech).

RT-RPA reactions were performed as instructed using TwistAmp® Basic (TwistDx) or RPA Basic Amplification Kit (ZC Bioscience), the total volume of amplification system was 10 μL for each reaction. The primers used in RPA were 600 nM for Y144 site, 400 nM for K417 site, and 200 nM for L452 site. Reactions were run with 1 μL (extracted RNA) or 2.5 μL (thermal lysed sample) of input template, 0.5 μL RiboLock RNase Inhibitor (Thermo) and 0.5 μL PrimeScript Reverse Transcriptase (PrimeScript RT, Takara) for 30 min at 40 °C. For specimens with low copy number, the volume of RPA system was

increased to 40 μL or 50 μL for each reaction, and other reagents were augmented correspondingly. For the blank sample, only buffer was used as input for amplification.

Amplicon digestion by Lambda Exonuclease

The amplified sample was digested into single stranded DNA (ssDNA) by Lambda Exonuclease (Lambda Exo, New England Biolabs Inc.)[36]. For each 10 μL of RPA system, the amplified sample was diluted to 50 μL with 1 μL Lambda Exo in 1 × reaction buffer, then incubated for 30 min at 37 °C. For RPA system with volume more than 10 μL, the upper limit for the digestion system was 100 μL with 2 μL Lambda Exo. The digested sample was diluted to 1 × TE buffer and 1 M NaCl. The mixture was denatured at 95 °C for 5 min, followed by quelling at 4 °C before being loaded onto FEMMAN chip.

Processing and imaging of FEMMAN-RPA assay

FEMMAN assay was performed as described previously. In brief, up to 150 μL of digested amplicon was applied to each set of DNA microarray in FEMMAN chip and incubated for 1 h to overnight. For the blank sample, amplification and digestion were also performed using DNase & RNase free water instead of template before being loaded to FEMMAN chip. After washing and blocking, the chip was incubated with IRDye800 labeled streptavidin in dark. All imaging was conducted using MidaScan-IR™ dual-channel confocal scanner with the 785 nm channel. The fluorescence intensity of each spot was analyzed by built-in software of the scanner with automatic spot identification.

Quantitative PCR (qPCR) analysis with TaqMan probes

To compare FEMMAN quantification with other established methods, we performed qPCR with diluted thermal lysed lentivirus and clinical samples. Quantitative reverse transcription polymerase chain reaction (qRT-PCR) was performed using a commercial kit targeting the ORF1b and N gene of SARS-CoV-2 (ShenZhen ZiJian Biotech Co., Ltd.). TaqMan probes of N501N or N501Y, and corresponding primer set (Supplementary Table 5) were designed according to Centers for Disease Control and Prevention of U.S. (CDC)[37] and synthesized by Sangon Biotech. Assays were performed using the HiScript II U+ One Step qRT-PCR Probe Kit (Vazyme) on a QuantStudio 5 (Thermo Fisher).

Digital droplet PCR (ddPCR) quantification

The concentration of viral RNA in reference material and thermal lysed lentivirus used in Figure 1, 3 was measured by ddPCR. The reference material for SARS-CoV-2 wild type genomic RNA was provided as 5.24×10^5 copies/μL, the reference material for SARS-CoV-2 Delta Variant (B.1.617.2) genomic RNA was provided as $(2.45 \pm 0.38) \times 10^3$ copies/μL, the lentivirus was provided as 4.88×10^5 copies/μL (Wild type), 5.38×10^5 copies/μL (Alpha), 1.13×10^6 copies/μL (Beta), 1.02×10^6 copies/μL (Gamma), 1.20×10^6 copies/μL (Delta), 7.04×10^5 copies/μL (Lambda), 6.59×10^6 copies/μL (Mu), and 2.26×10^3 copies/μL (Omicron).

Sanger sequencing preparation

Extracted viral RNA was prepared for Sanger sequencing. Following extraction, double-stranded complementary DNA (cDNA) was created and amplified using Spike protein primers (Supplementary Table 5) and PrimeScript™ One Step RT-PCR Kit (Takara). Sequencing was performed by Sangon Biotech.

Data analysis

General data analysis

The background subtracted fluorescence intensity for each spot was counted by the analysis software of scanner and the mean of the triplicate spots was taken for further analysis. All spots were divided into three groups (G142-Y145, K417, and L452) according to the corresponding primer pairs. Imaging data was analyzed with built-in software of the scanner. To calculate background subtracted fluorescence data, the fluorescence signal around the spot was subtracted as background to allow for comparisons between different assays. The averaged background subtracted fluorescence intensity of each probe would be normalized to positive control spot in each block.

Statistical analysis

The signal proportion of each wild type or mutation site was calculated as follows:

$$Probe\ A_k\ ratio = \frac{MFI_{A_k}}{\sum_{i=1}^{m} MFI_{A_i}}$$

Where MFI_{A_k} refers to the mean value of fluorescence intensity for probe A_k, m refers to the number of probes for the same target site (G142-Y145, K417, or L452), and A_i refers to the probes in the same target site (Fig. 4e). Take Y144Y as example:

$$Probe\ Y144Y\ \ ratio = \frac{MFI_{Y144Y}}{MFI_{Y144Y} + MFI_{Y144del} + MFI_{Y144SY145N} + MFI_{G142D143-145del}}$$

Heat map was generated from the proportion of the mean fluorescence intensity of each probe in group (Fig. 4f). In the heat map of Fig. 3e, mutation indexes were normalized by column.

SARS-CoV-2 detection of clinical samples

Background subtraction and normalization were performed as in general data analysis. For each sample, the signal of each target site (G142-Y145, K417, or L452) was calculated as follows:

$$MFI_A = \sum_{i=1}^{m} MFI_{A_i}$$

Where A refers to G142-Y145, K417, or L452 target site, MFI_A refers to the mean value of fluorescence intensity for target A, m refers to the number of probes in target A, and A_i refers to the probes in target site A.

For each target site, the threshold for SARS-CoV-2 viral RNA detection in FEMMAN-RPA assay was defined at 3 × s.d. above the MFI_A value (MFI_{Y144}, MFI_{K417} and MFI_{L452}) of blank (dotted box in Fig. 4b).

Methods-only References

33 Dovgan, I., Kolodych, S., Koniev, O. & Wagner, A. 2-(Maleimidomethyl)-1,3-Dioxanes (MD): a Serum-Stable Self-hydrolysable Hydrophilic Alternative to Classical Maleimide Conjugation. *Sci. Rep.* **6**, 30835, doi:10.1038/srep30835 (2016).

34 Wei Wang, M. W. V. Morphology and amine accessibility of (3-aminopropyl) triethoxysilane films on glass surfaces. *30* **2**, 13, doi:10.1002/sca.20097 (2008).

35 Deb-Choudhury, S., Plowman, J. E. & Harland, D. P. Isolation and Analysis of Keratins and Keratin-Associated Proteins from Hair and Wool. *Methods Enzymol.* **568**, 279-301, doi:10.1016/bs.mie.2015.07.018 (2016).

36 Deng, J. *et al.* Targeted bisulfite sequencing reveals changes in DNA methylation associated with nuclear reprogramming. *Nat. Biotechnol.* **27**, 353-360, doi:10.1038/nbt.1530 (2009).

37 Matic, N. *et al.* Rapid Detection of SARS-CoV-2 Variants of Concern, Including B.1.1.28/P.1, British Columbia, Canada. *Emerg. Infect. Dis.* **27**, 1673-1676, doi:10.3201/eid2706.210532 (2021).

Declarations

Ethics statement

Human samples from patients with SARS-CoV-2, coronavirus HCoV-NL63 and HCoV-OC43, influenza A virus H3N2 and H1N1, Influenza B virus Yamagata and Victoria lineages, adenovirus serotype 3, 7, and 55 were obtained from Shenzhen Third People's Hospital under ethical approvals (Approval No. 2021-030). All protocols performed subsequently were approved by the Institutional Review Boards of Southern University of Science and Technology and Shenzhen Third People's Hospital (Approval No. 2021SYG021).

Acknowledgments We thank members of the Yongye Liang laboratory for helpful discussions and amplification site. We also thank Jian Ding, Zhanning Liu, Zhongrong Tang, Yifei He, Yiyi Liu, Shuang He,

Tingzhen He, Bingyun Wang, Shinong Zeng, Jingxiang Xu, Wei Wang, Xin Li, Jianhao Sheng, Yijie Wang, Haipeng Wang, Zhan Jiang, Wenhui Xie, Mingshun Cheng, Mingkai Zhai, Yunye Tian, Jiahao Ming, Xinrui Gong, and Zhichao Lin for negative samples collection; Feng Yang and Xin Zhao for assistance in SEM imaging. This work is supported by Shenzhen Science and Technology program project (No. JCYJ20180504165657443 and JCYJ20210324104007020), Guangdong Basic and Applied Basic Research Foundation (No. 2022A1515011408), and Key Research and Development Program (No. 2021YFC2301803).

Author contributions B.Z. and Y.L. conceived of the study and designed the experiments. Y.L., G.W. and R.H. performed the assay experiments. J.L. performed the SEM imaging. Y.Y., Y.L., J.Y., P.S., H.X., J.Y., D.N., Y.H., Z.X. and J.Y. collected the clinical samples, Y.Y. performed the viral RNA extraction and thermal lysis of clinical samples. Y.L., J.T., M.T., H.D and B.Z. analyzed the data and wrote the manuscript. Y.L., Y.Y. and G.W. contributed equally to this work. All authors participated in experimental data/results analysis and discussion.

Competing interests declaration H.D. is a scientific adviser for Nirmidas Biotech Inc. and contributed to this work in that capacity independent of his Stanford work. The authors declare no other competing interests.

Supplementary Information is available for this paper. Correspondence and requests for materials should be addressed to B. Zhang (zhangb3@sustech.edu.cn), H. Dai (hdai@stanford.edu) J. Yuan (yuanj2020@mail.sustech.edu.cn) or M. Tang (meijie.tang@nirmidas.com). Reprints and permissions information is available at www.nature.com/reprints.

Data availability The datasets generated during and/or analyzed during the current study are available from the corresponding author on reasonable request.

Figures

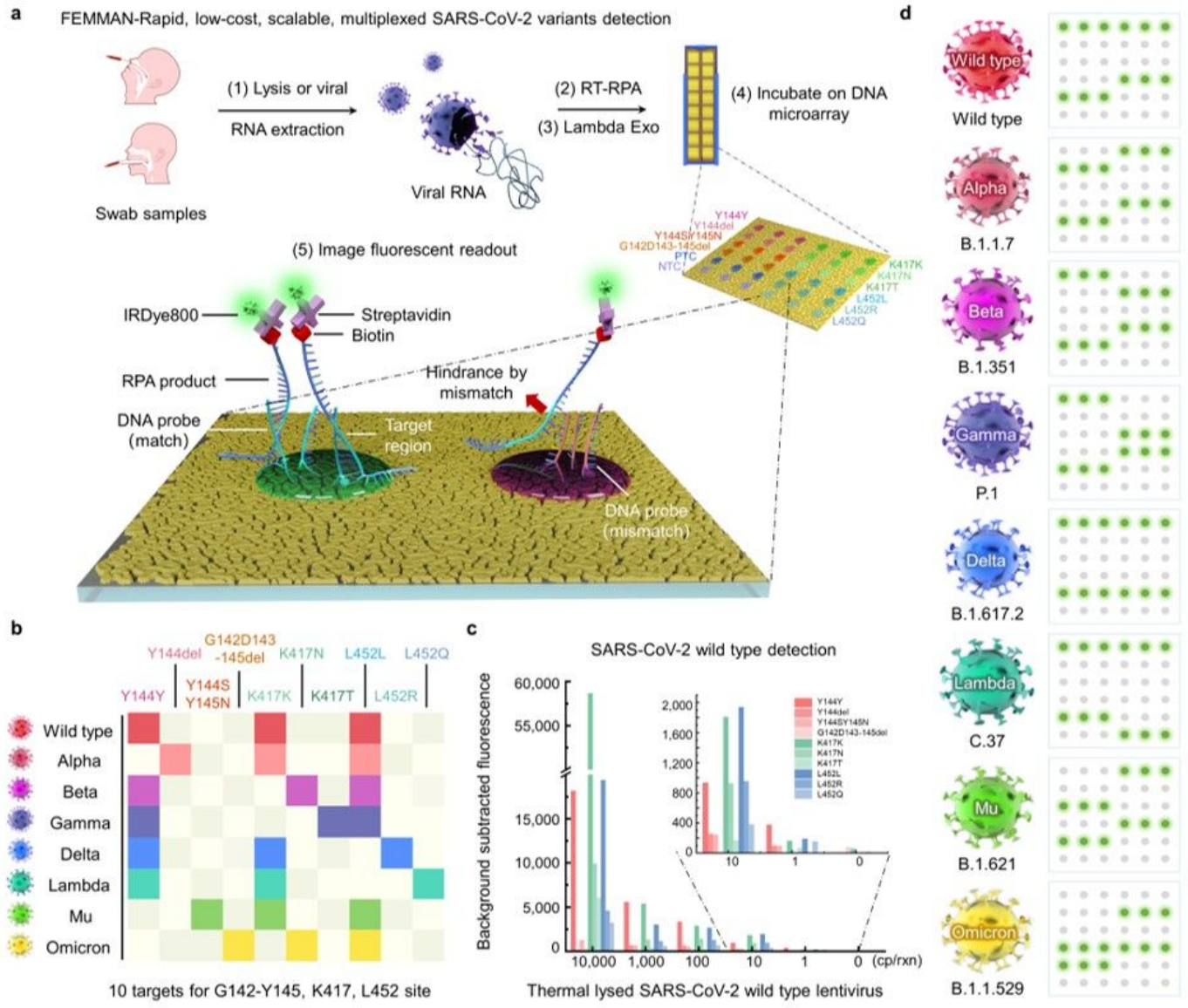

Figure 1

FEMMAN achieves single-RNA copy sensitivity with RT-RPA in SARS-CoV-2 detection and simultaneous variants discrimination with SNV distinction. a, Schematic of FEMMAN-RPA workflow. SARS-CoV-2 related DNA probes (Y144Y, Y144del, Y144SY145N, G142D143-145del targeting G142-Y145 site, K417K, K417N, K417T targeting K417 site and L452L, L452R, L452Q targeting L452 site), a terminal biotin labeled DNA probe as positive reference, and a DNA probe unrelated to SARS-CoV-2 as negative control were arrayed on the plasmonic gold substrate in the listed order. The viral RNA, released by thermal lysis or RNA extraction, was amplified by RT-RPA with following digestion by Lambda Exo. Without further purification step, the amplified sample diluted in binding buffer was directly loaded to FEMMAN chip, following with identification by IRDye800 labeled streptavidin. **b**, Schematic for heat map of fluorescence intensity statistics for different SARS-CoV-2 lineages. **c**, SARS-CoV-2 (wild type) identification by FEMMAN-RPA assay with single-molecule sensitivity and SNV distinction. **d**, Schematic for representative

chips image of 8 SARS-CoV-2 lineages (wild type, Alpha, Beta, Gamma, Delta, Lambda, Mu and Omicron) by FEMMAN-RPA assay. The positive reference in each block served as inter-block signal normalization.

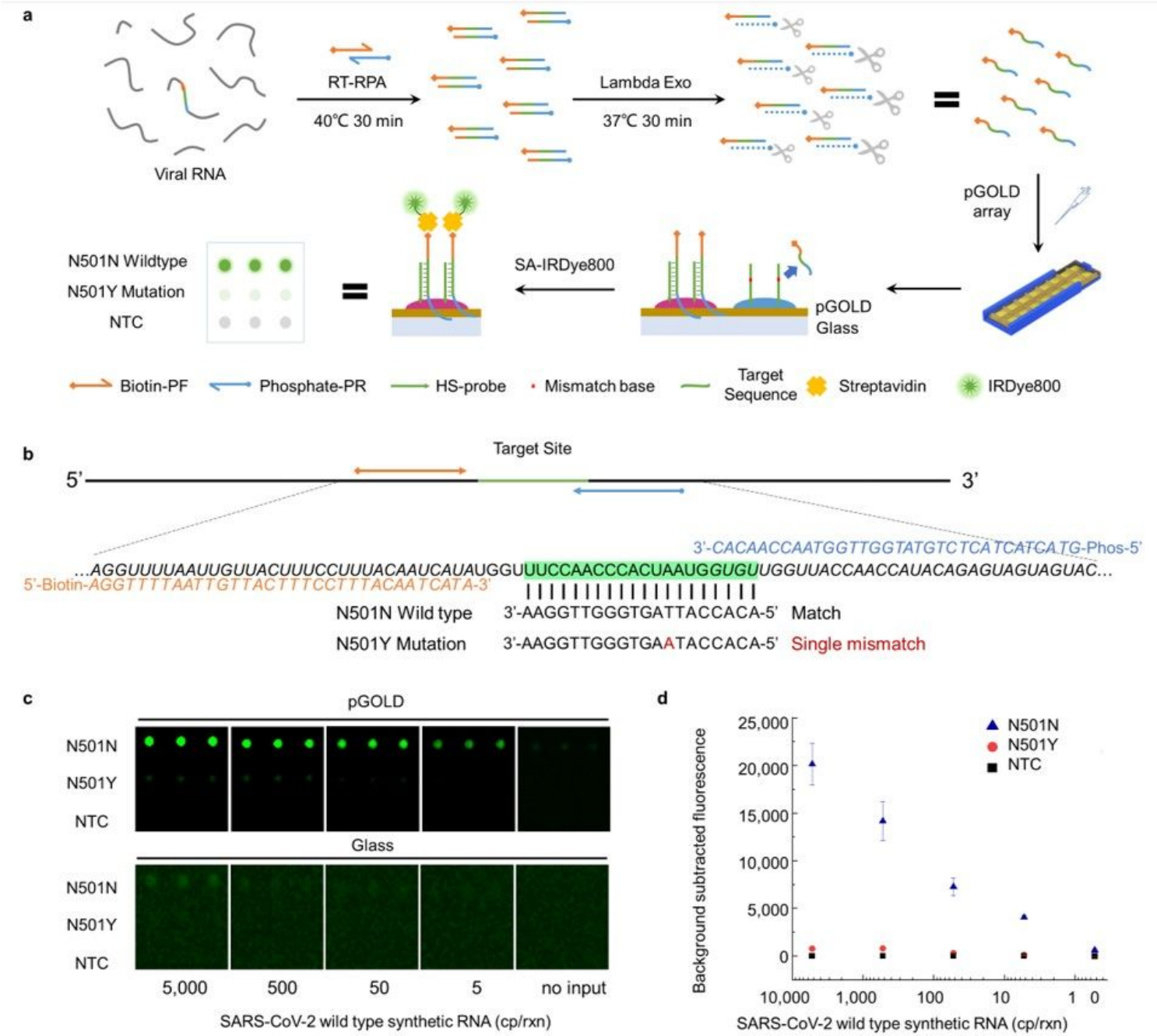

Figure 2

FEMMAN-RPA workflow at the molecular scale and titration curve for SARS-CoV-2 detection. a, Detailed molecular schematic of SARS-CoV-2 viral RNA detection using FEMMAN-RPA assay. N501N, N501Y probes and negative control (NTC) were arrayed on pGOLD substrate. After amplification by RT-RPA with 5'-biotin labeled forward primer (Biotin-PF) and 5'-phosphorylated reverse primer (Phosphate-PR), the amplicon was digested by Lambda Exo to gain single-stranded amplicon with 5'-biotin tag. After binding to immobilized DNA probes, the amplicon with biotin tag would be identified by NIR IRDye800 labeled streptavidin. The chips were imaged by the scanner with 785 nm wavelength channel. **b**, Sequences of

the DNA probes and primers for N501 target site. The target site is highlighted in green. **c**, IRDye800 fluorescence images of a typical titration curve for SARS-CoV-2 wild type viral RNA detection by FEMMAN-RPA from 5,000 copies/rxn to 5 copies/rxn on pGOLD and glass substrate. **d**, Background subtracted fluorescence quantification of viral RNA titration on pGOLD for N501N, N501Y and NTC probes.

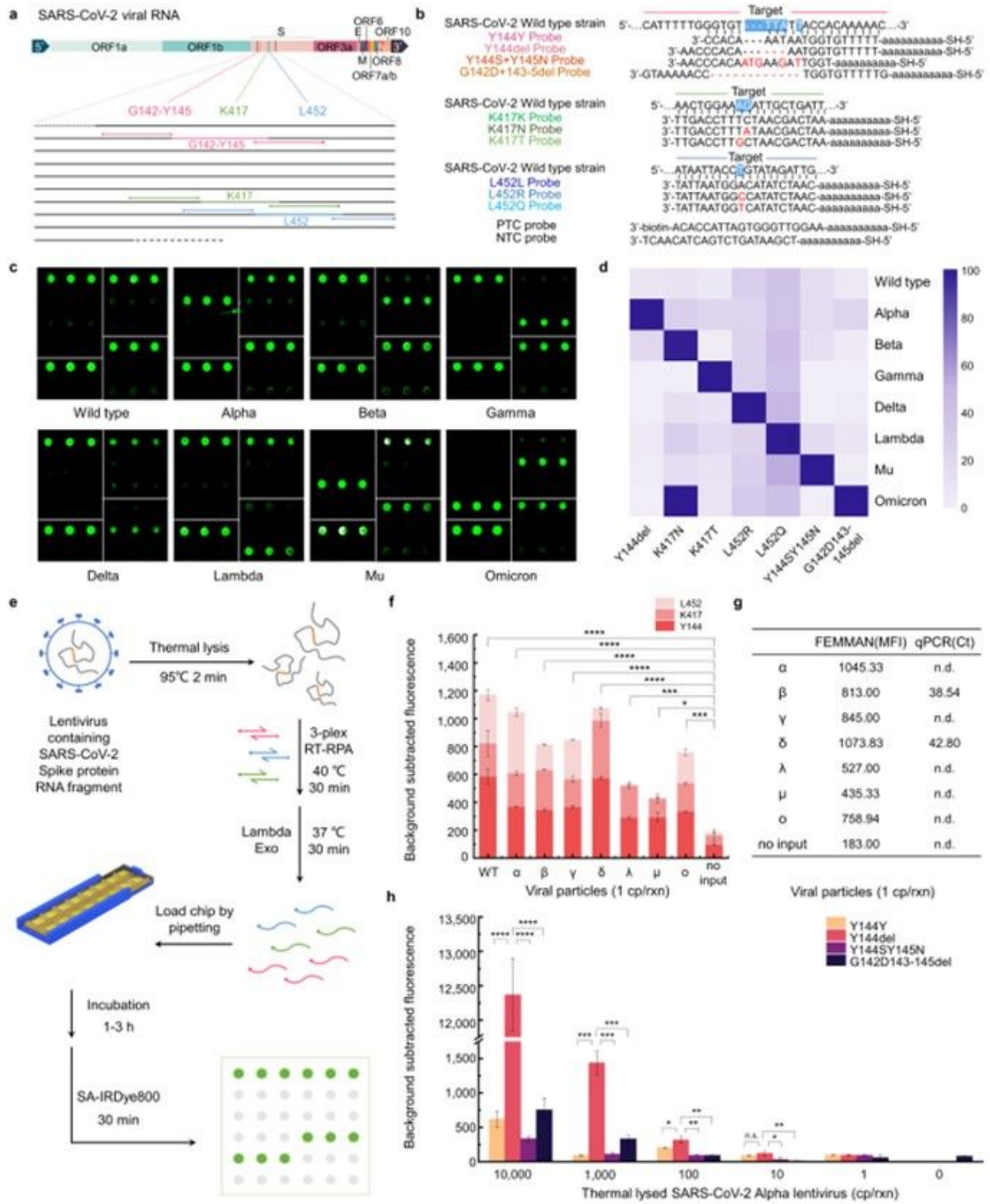

Figure 3

Comprehensive identification of SARS-CoV-2 lineages by FEMMAN-RPA. a, Schematic of target sites (G142-Y145, K417, L452) in SARS-CoV-2 viral RNA and primer pairs designed for multiplex RPA. **b**, Sequences of DNA probes in SARS-CoV-2 panel. **c**, IRDye800 fluorescence images of SARS-CoV-2 lineage identification by FEMMAN-RPA with RNA extracted from lentiviruses. Block in top left corner represented G142-Y145 target site, block in top right corner represented K417 target site, block in right bottom corner represented L452 target site, and block in left bottom corner represented positive reference and negative control. **d**, Heat map for discrimination of SARS-CoV-2 wild type, Alpha, Beta, Gamma, Delta, Lambda, Mu and Omicron using extracted RNA of lentiviruses. The signal proportion of each mutation site was calculated as follows: MFI (mutation) / [MFI (wild type) + MFI (mutation 1) + ... + MFI (mutation n)], and the results would be normalized to the maximum as 100. **e**, Schematic of SARS-CoV-2 detection by FEMMAN-RPA without viral RNA extraction for point-of-care testing. **f**, FEMMAN-RPA assay achieved single-molecule sensitivity post amplification for SARS-CoV-2 detection of 8 lineages without viral RNA extraction. **g**, Comparison between FEMMAN-RPA and qPCR in single copy detection with thermal lysed lentiviruses. **h**, Alpha variant identification in G142-Y145 site by FEMMAN-RPA from 10,000 copies/rxn to 1 copy/rxn. In **c** and **d**, extracted target RNA fragments were applied at 1,000 copies per reaction, measured by ddPCR. In **f**, **g** and **h**, the input of RT-RPA was thermal lysed lentivirus. n = 3 technical replicates, two-tailed Student's *t* test; *$P < 0.05$, **$P < 0.01$, ***$P < 0.001$, and ****$P < 0.0001$; MFI, mean fluorescence intensity; n.s., not specific; n.d., not detected; bars represent mean ± SEM.

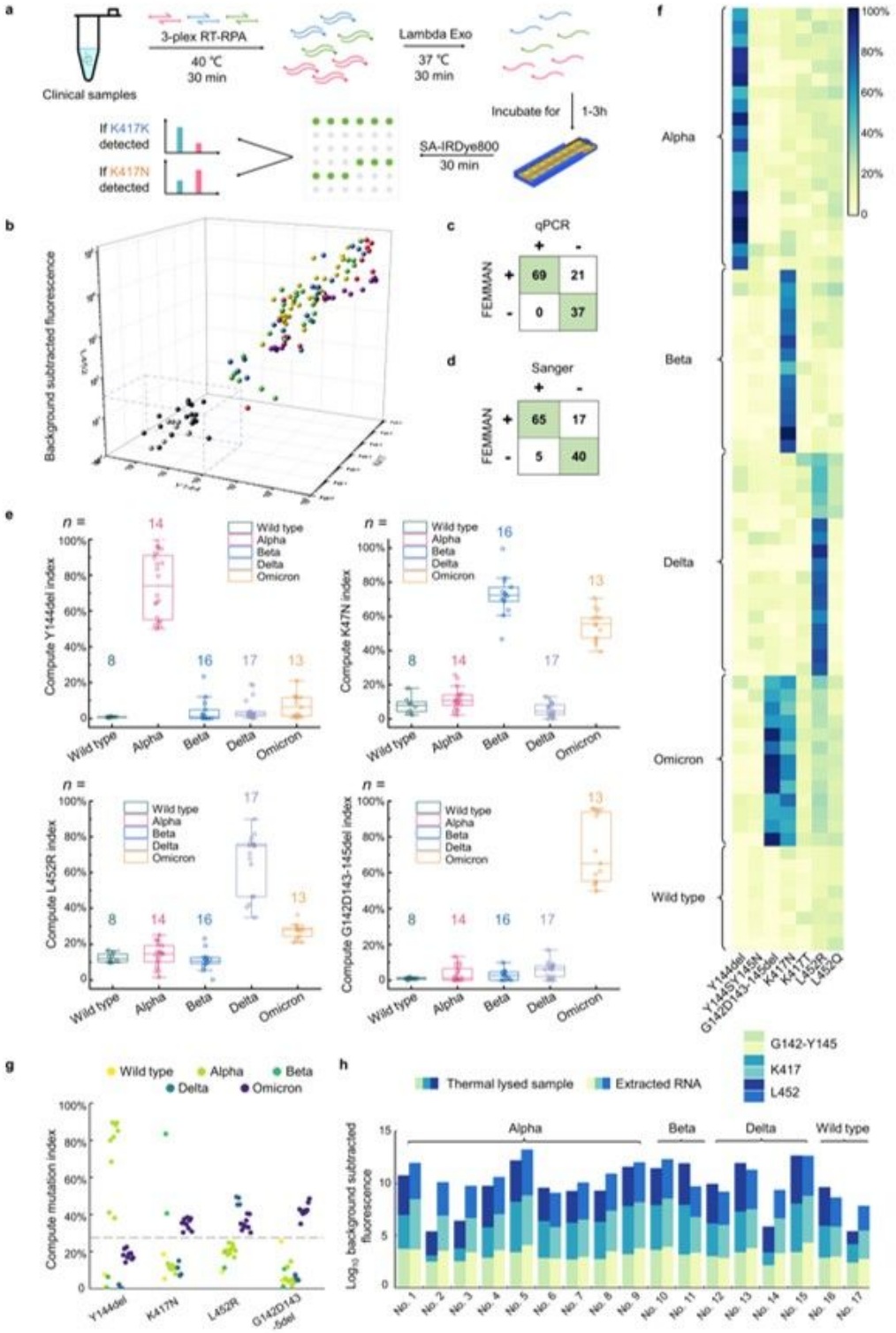

Figure 4

SARS-CoV-2 detection and viral lineage discrimination of clinical samples with FEMMAN-RPA. a, Schematic for SARS-CoV-2 detection and viral lineage identification using FEMMAN-RPA. **b**, Positive/negative assessments of 127 clinical samples. The dotted line represents fluorescence intensity threshold of 3 × s.d. above blank. Dots in black for uninfected individuals, grey for non-SARS-CoV-2 HVs-infected patients, red for SARS-CoV-2 wild type, yellow for Alpha, blue for Beta, green for Delta, purple for

Omicron. **c**, Sensitivity concordance between FEMMAN-RPA and qPCR, of which the results with Ct value > 35 were identified negative. **d**, Specificity concordance between FEMMAN-RPA and Sanger sequencing. **e**, Signal proportion calculation of Y144del, G142D143-145del in G142-Y145 site, K417N in K417 site, and L452R in L452 site for 72 positive samples identified by FEMMAN-RPA with extracted RNA. **f**, Heat map indicates SARS-CoV-2 lineage discrimination of 72 positive samples identified by FEMMAN-RPA with extracted RNA. **g**, Signal proportion calculation of Y144del, G142D143-145del in G142-Y145 site, K417N in K417 site, and L452R in L452 site for 27 positive samples with thermal lysed nasopharyngeal swab samples. **h**, Concordance between thermal lysis (up) and RNA extraction (below) for 17 positive samples obtained in both forms.

Supplementary Files

This is a list of supplementary files associated with this preprint. Click to download.

- FEMMANSI.docx
- FEMMANExtendedData.docx